

PACS numbers: 95.30.Dr; 95.30.Ky; 42.55.–f
DOI: 10.1070/QE2002v032n12ABEH002349

Astrophysical lasers

V.S. Letokhov

***Abstract*. A review of lasers operating under natural astrophysical conditions is presented. A principal difference between the conditions for obtaining inversion and amplification in an astrophysical laser and in well-known astrophysical masers is considered. The data for a recently discovered Fe II ion astrophysical laser are presented. The parameters of the astrophysical laser amplifier are discussed and the possibility of its conversion into the astrophysical laser with the incoherent feedback is considered, as well as the methods for studying the width of the emission spectrum of the astrophysical laser.**

Keywords: *astrophysical lasers and masers, incoherent feedback, inverted population.*

1. Introduction

The principles of operation of masers and lasers were discovered during a decade between 1950 and 1960 in the first independent and then interrelated investigations performed at the P.N. Lebedev Physics Institute, Russian Academy of Sciences, and at the Columbia University (USA). These fundamental pioneering studies received the highest international recognition [1]. The experimental demonstration of lasers [2, 3] and the subsequent exponential progress both in the development of lasers themselves and their applications confirmed a great scale of this discovery. The role of N.G. Basov in this progress is unique because he and his disciples were in the forefront of a rapid development of quantum electronics for a few decades. However, in fact all these advances are only the beginning of the 'laser century' because a real scale of the mastering of the optical range by coherent sources of electromagnetic radiation will be manifested in full measure only in the XXI century.

It is fairly interesting to consider the origin of quantum electronics, which has appeared due to the development and synthesis of two trends in physics: classical electromagnetic physics (we will call it 'the radio trend') and quantum physics (we will call it 'the optical trend') because quantum physics was created based on atomic physics and optical spectroscopy and then became the foundation of physics as a whole). Both these trends are combined by Maxwell's equations.

Fig. 1 shows the selective sequence of key discoveries, ideas, and experiments, which resulted in the creation of quantum electronics. The main sequence of events, which have led to the discovery of a laser, is shown by the solid arrows, while the possibilities of the discovery of a laser by amplifying light in a medium with the inverted level population that have not taken place are shown by the dashed arrows. Although lasers could be discovered along the optical trend, in reality they were discovered only after

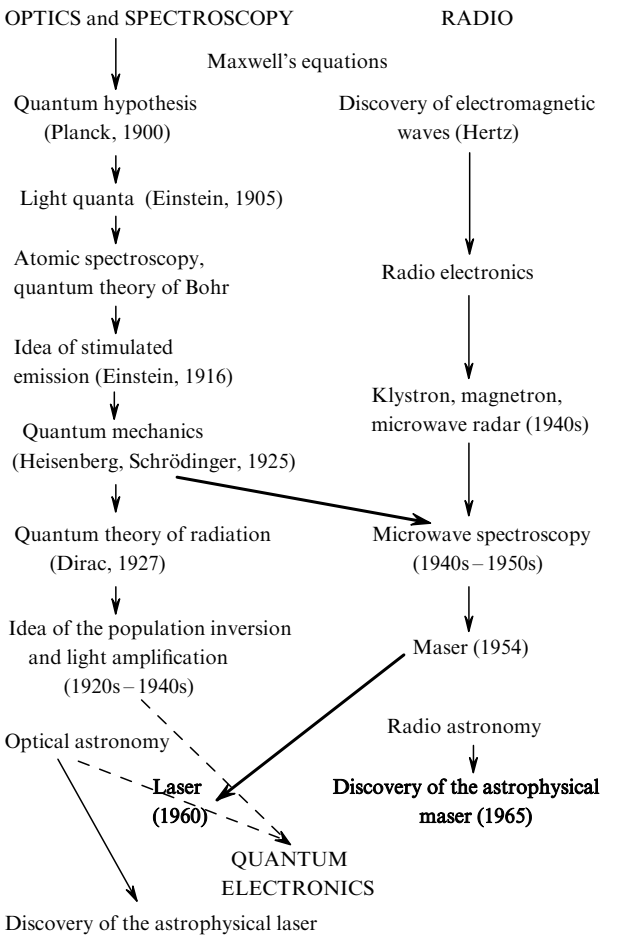

Figure 1. Sequence of discoveries in optics and radio resulting in the birth of quantum electronics.

V.S. Letokhov Institute of Spectroscopy, Russian Academy of Sciences, 142190 Troitsk, Moscow region, Russia; e-mail: letokhov@isan.troitsk.ru

Received 4 July 2002
Kvantovaya Elektronika **32** (12) 1065 – 1079 (2002)
Translated by M.N. Sapozhnikov

the creation of a maser, i.e., due to the progress in the radio trend. At first the concepts of quantum physics and the creation of microwave sources of electromagnetic radiation for radars led to the development of radiospectroscopy, and then masers (molecular generators) were created. And only thereafter the extension of the concept of the cavity feedback to the optical region, where the idea of the inverted population of energy levels involved in optical transitions was proposed long ago, resulted in the creation of a laser. This confirms once more an extremely important role of the interrelation and synthesis of various fields of science and technology in the scientific and technical progress. Although lasers could be discovered independently of the radio trend, this did not happen, which again confirms the inevitability of the discovery itself despite the fact that its specific scenario is unpredictable and always has its own personal and subjective aspect.

In this connection, it is interesting to call attention to the fact that natural masers operating under astrophysical conditions on the OH radical at $\lambda = 18.5$ cm [4] and on the H_2O molecule at $\lambda = 1.35$ cm [5] were discovered in radio astronomy in the mid-1960s, ten years after the creation of first laboratory masers in Moscow and New York.

Because the brightness temperature of the microwave radiation of astrophysical masers is as high as $10^{12} - 10^{18}$ K, it can be explained only by the amplification due to stimulated emission in a medium with the inverted population of low-lying molecular levels. This was another scenario of a discovery that could be made earlier. Astrophysical lasers emitting in the optical range, which are discussed in this paper, were discovered quite recently, forty years after the creation of the laboratory laser. However, their roots can be traced as early as 1930s – 1940s, i.e., long before the creation of lasers and masers. In those years, astrophysicists explained the appearance of anomalous spectral emission lines (pump lines) of an element by their coincidence with the absorption line of another element (the accidental Bowen coincidence [6, 7]). They also used the relations for the pump and emission rates, which are equivalent in the modern terms to the condition of the inverted population [8] (see Section 3). This is also another unrealised scenario of the discovery of the laser action based on astrophysical observations.

2. Operation conditions for the astrophysical laser*

Electromagnetic radiation can be amplified by an ensemble of quantum particles only when the thermodynamic equilibrium is strongly violated, i.e., when at least one of the following equilibrium conditions is violated:

(i) The equilibrium Boltzmann distribution of the population of the quantum states of particles in the ensemble or of the average squares of the amplitudes of the wave functions of states.

(ii) The equilibrium state of the electromagnetic radiation in which an ensemble of particles with a given equilibrium temperature is located, which is equivalent to the absence of external radiation except the equilibrium radiation of the ensemble.

(iii) The equilibrium (random) distribution of phases of the wave functions of quantum states, i.e., the absence of the average nonzero (non-fluctuation) polarisability or coherence in the ensemble.

The violation of the first condition, resulting in the population inversion for some pair of levels, can be achieved by many methods, for example, upon selective incoherent pumping of an excited level in the three- or four-level scheme (Figs 2a, b, respectively). For this reason, it is used virtually in all lasers [9].

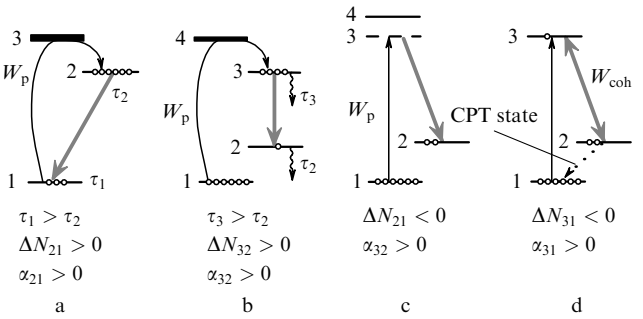

Figure 2. Various methods for obtaining amplification, based on producing the population inversion in three-level (a) and four-level (b) schemes, by means of Raman scattering without the population inversion (c), and using the coherent superposition of the states 1 and 2 without the population inversion for the levels 2 and 3 (d). To obtain amplification in schemes (a) and (b), incoherent pumping with a moderate rate [especially in the scheme (b)] is required. To obtain amplification in scheme (c), pumping with a very high spectral intensity is required (not necessarily coherent). To obtain amplification in scheme (d), coherent pumping at the $3 \rightarrow 1$ transition is required and CPT states 1 and 2 should be present.

A strong violation of the second equilibrium condition can cause amplification even without the population inversion. The example is a Raman laser [10] when a transparent medium in a strong laser field becomes amplifying at the Stokes frequency of Raman scattering in a medium with the equilibrium population of levels only due to the presence of intense monochromatic radiation in the ensemble (Fig. 2c)*. Note that in this case, laser radiation should be only intense and could have a broad spectrum (of the order of the Raman linewidth), whereas its high coherence does not required.

When amplification is produced by violating the first and second equilibrium conditions, the active medium is in an incoherent state, which is natural because the phase relaxation time in an ensemble is usually much shorter than the population relaxation time. Coherence is produced only by placing the active medium into an optical cavity, which selects a finite number of spatial modes, in which a high rate of stimulated emission is maintained. In other words, the coherence of radiation is produced spontaneously due to the 'phase transition' in the active medium + intracavity radiation system [11].

A substantially different situation takes place in the case of the third equilibrium condition, which can be violated only when special measures are taken. The equilibrium

* We call an astrophysical laser amplifier the astrophysical laser (APL). Conditions under which the APL is transformed to a generator due to an incoherent feedback produced by scattering are discussed in Section 8.

* We do not consider the possibility of inversionless amplification due to the recoil effect, when emission and absorption lines have different frequencies. Free relativistic electron lasers are a spectacular example of such a situation.

(random) distribution of phases (more exactly, phase difference) of the wave functions of some two quantum states can be violated under the action of an external coherent field, which matches the phase difference of the wave functions of two states interacting with this field (one- or two-frequency). Due to such a matching, a quantum system in the ensemble can be prepared in a superposition antisymmetric state of two stationary quantum states (1 and 2 in Fig. 2d). Such a state is called a coherently population trapped (CPT) state [12, 13]. A particle in the CPT state absorbs radiation neither at the $1 \rightarrow 2$ transition nor at the $2 \rightarrow 3$ transition (the $1 \rightarrow 2$ transition is assumed forbidden) because of the quantum destructive interference of two counter quantum transition routes $1 \rightarrow 3 \rightarrow 2$ and $2 \rightarrow 3 \rightarrow 1$. This effect is related to the electromagnetically induced transparency [14], when a coherent electromagnetic field produces the CPT state from which radiation is not absorbed. This effect was used to demonstrate the inversionless laser operating due to the violation of the third equilibrium condition in the Λ scheme shown in Fig. 2d [15] and in the V scheme [16].

The first equilibrium condition can be easily violated under astrophysical conditions. In this case, the inverted population appears due to the spatial inhomogeneity of the density, temperature and other parameters of the astrophysical medium (stars and gas clouds near them, etc.), when the medium is in a stationary but not an equilibrium state. By discussing this possibility for astrophysical media, we should consider separately the pulsed [2] and continuous quasi-stationary [3] regimes for producing the population inversion. In the pulsed regime, the pumping rate of a level should exceed its relaxation rate, which for optical transitions is usually greater than 10^{-3} s^{-1} (while for forbidden transitions, the relaxation rate sometimes achieves 1 s^{-1}). Under astrophysical conditions, this situation is unlikely because the characteristic times of pulsed astrophysical phenomena, which can be used for pumping, are much longer than the population relaxation times for quantum particles.

In the continuous (quasi-stationary) laser regime, the effect of a faster relaxation of the lower level of the lasing transition compared to that of the upper level is used [3] (Fig. 2b). In this case, inversion always exists on such a transition, and the pumping rate should provide a certain density of the population inversion for the levels, which is required for obtaining the threshold amplification. This regime is used in all cw lasers, and seems the most probable for astrophysical lasers, as was assumed in Ref. [17]. It is realised most readily when the radiative lifetimes of the two corresponding levels are substantially different (in an appropriate way). In this case, the inverted population appears in an isolated quantum system without any collisions, which is typical for rarefied gaseous circumstellar or interstellar matter). The astrophysical laser operating according to this scheme on the highly lying levels of Fe II at a wavelength of ~ 1 μm was discovered recently in a gas condensate in the vicinity of the most massive and bright star η Car of our galaxy [18].

However, although collisions of particles at higher densities in stellar atmospheres return the ensemble of particles to the equilibrium state, these collisions can also play a positive role due to a predominantly collision depletion of the lower level. Strange as it may seem, but the role of collisions in the enhancement of the intensity of emission lines in stellar atmospheres according to the typical laser scheme [19] was discussed in astrophysical papers even in 1930s [8]. Because in these papers the questions related to stimulated emission were discussed, they are considered separately in Section 3.

To violate the second equilibrium condition, an intense monochromatic excitation is required, which can usually be generated only by a laser. A Raman line is always amplifying, with the gain proportional to the intensity of external radiation within the Raman line width. Only one observation of Raman scattering is known under astrophysical conditions. In [20], Raman scattering of the O VI line at $\lambda = 1032$ and 1038 Å by the $1S - 2P$ electronic transition in neutral hydrogen H I (close to the resonance with the Ly_α Lyman line of H I at 1026 Å) was observed. Due to such scattering, the hydrogen atom was found in the $2S$ state and the Raman line was observed in the visible region (at 6825 and 7082 Å). This effect was observed under special astrophysical conditions of symbiotic stars where strong VUV emission lines of highly ionised atoms irradiate the high-density regions of neutral hydrogen. The gain at Raman lines is rather low, and only spontaneous scattering can occur.

The spontaneous (without any coherent field) violation of the third equilibrium condition, i.e., the condition of a random distribution of the phase difference of the wave functions of quantum states of independent particles in the ensemble seems unlikely. (The only exception is an ensemble of an ultracold gas of boson atoms of a sufficient density, where the Bose-Einstein condensation is observed.) Nevertheless, the authors of paper [21] put forward a bold hypothesis about the possibility of inversionless amplification under astrophysical conditions at a Balmer line in hydrogen (at the $3P - 2S$ transition). The relaxation of the phases of quantum states in rarefied gases (of density lower than 10^8 cm^{-3}) indeed can occur very slowly (for minutes and longer), while in the excited $2S$ state of H I it occurs for 0.12 s (because of spontaneous two-photon decay). However, to produce coherence of the $1S$ and $2S$ states (or, more exactly, CPT states) of hydrogen, the mechanism of spontaneous appearance of the CPT state should exist. The authors of paper [21] assume that such a process can be induced by two intense incoherent emission lines, the 1215-Å Ly_α line and the 6563-Å H_α Balmer line upon spontaneous decay of the excited state of an atom over two completely different and quite discernible channels, although its probability is extremely low. It would be very interesting to detect this process, because this is an example of an unusual phase transition of an ensemble of quantum particles from the incoherent state to the coherent one. At present, only one example of such a phase transition is known, when an amplifying incoherent laser medium is placed in an open resonator, which drastically restricts the number of spatial modes of stimulated emission, i.e., makes a 'coherent' ensemble.

3. Astrophysical predecessors of the laser*

Astrophysics was the main driving force of atomic spectroscopy in the last century because the astronomical spectra of stars, nebulae, and galaxies gave the main

* The material of this section is based on report [17], which was published only as preprint no. 9 of the Institute of Spectroscopy, Russian Academy of Sciences (Troitsk, 1972).

information on the structure and development of the Universe. The spectroscopy of stellar atmospheres has received the most study [22].

The emission of a star detected by an observer represents the continuous emission of the photosphere, which propagated through the stellar atmosphere enveloping the photosphere, and the line emission of the stellar atmosphere. Therefore, depending on whether absorption or spontaneous emission dominates, the discrete absorption or emission lines of the stellar atmosphere are observed against the background of the continuous spectrum of the photosphere. If the photosphere emission is very intense, while the brightness of spontaneous emission of the atmosphere is low, discrete absorption lines are observed. This situation is typical for most usual stars.

However, the spectra of many stars contain bright emission lines [23]. This is possible if the atmosphere-emission intensity at the corresponding wavelength is comparable with the intensity of the continuous emission spectrum of the photosphere at this wavelength. For this reason, bright lines can be observed only in the spectra of stars having extensive atmospheres or the photosphere with a comparatively weak emission. The bright emission lines are very often observed in the spectra of unstable (variable) or binary stars [24].

Three mechanisms are mainly used to explain the observation of bright emission lines [22, 24]: collision excitation, excitation due to recombination, and the original mechanism of fluorescence excitation, which is based on an accidental coincidence of a strong emission line of one element with an absorption line of another element [6, 7]. However, in some cases these mechanisms cannot explain so far the anomalous intensities of emission lines in stellar spectra.

It was pointed out in Ref. [17] that some anomalous bright emission lines could be explained by stimulated emission in the stellar atmosphere due to the inverted population of the levels involved in optical transitions. Consider most typical anomalies, which were explained in papers [7, 8]. The authors of these papers came up with the ideas, which are, in my opinion, the early predecessors of the concept of obtaining an amplifying laser medium by producing the inverted population of the corresponding levels.

It is known that the O I emission lines of oxygen at 7774 and 8446 Å in the spectra of the Be stars (the earlier stars of the spectral class B with emission lines) exhibit the anomalous behaviour [23, 25]. The ratio of the intensities of the 8446-Å ($3p\,^3P \rightarrow 3s\,^3S^0$) and the 7774-Å ($3p\,^5P^0 \rightarrow 3s\,^5S^0$) lines is much greater than the laboratory value. Bowen assumed [26] that this is explained by fluorescence caused by the coincidence of the bright Ly_β H I line (1025.72 Å) with the absorption line of O I at 1025.77 Å ($2p\,^3P \rightarrow 3d\,^3D^0$). The scheme of these transitions in O I is presented in Fig. 3a. If this assumption were true, then not only the 8446-Å line but also the 11287-Å line of the $3d\,^3D^0 \rightarrow 3p\,^3P$ intermediate transition in the cascade transition would be bright. However, nothing of the kind has been observed in stellar spectra [23]. In addition, to explain the observed intensities of the hyperfine-structure components of the 8446-Å line in the line-coincidence model, it is necessary to assume that the velocities of the regions of the line emission and absorption greatly differ (up to 85 km s^{-1}) to provide the Doppler shift compensating for the difference between the frequencies of the emission and absorption lines [27].

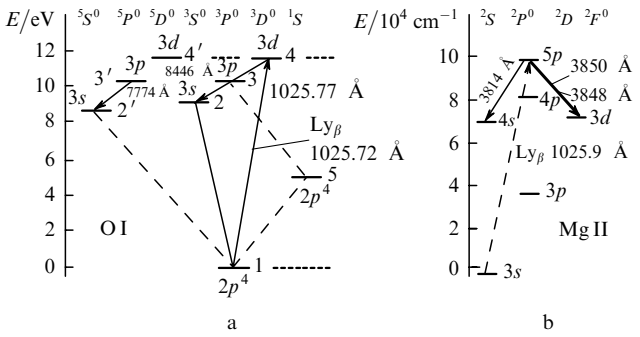

Figure 3. Astrophysical excitation schemes of the levels of O I (a) and Mg II (b) by Ly_β emission of H I explaining the appearance of bright lines at 8446 Å (O I) and 3848 Å (Mg II).

The anomalous ratio of the line intensities can be explained by stimulated emission due to the population inversion at the 8446-Å transition. Because the lower $3s\,^3S^0$ level of the transition has a shorter lifetime than the upper $3p\,^3P$ level, the inversion can be achieved upon moderate cw pumping of the upper level [17]. Laser action in stellar atmospheres and nebulae (at $\lambda = 8446$ Å) is considered in Section 6.

An example of a similar anomaly is the Mg II lines at 3848 and 3850 Å ($5p\,^2P^0 \rightarrow 3d\,^2D$) of the same multiplet (Fig. 3b). The first line can be sometimes much brighter than the second one [23, 28]. Attempts were made to explain this anomaly by the coincidence of the 1025.87-Å ($3s\,^2S \rightarrow 5pP_{3/2}$ absorption line of Mg II with the 1025.7-Å Ly_β emission line of hydrogen. However, the absence of the anomaly for another line at 3614 Å with the same upper level ($5p\,^2P^0 \rightarrow 4s\,^2S$) casts doubt on this mechanism [23].

The intensity anomalies are most often observed in the spectra of long-period variable stars of late spectral classes (M and S stars). The certain multiplets are often observed in emission in which the relative intensities of lines differ from their laboratory values [29]. An example is the anomalous behaviour of the 4101.72-Å and 4511-Å lines of In I observed upon transitions between the lower terms (Fig. 4a). The 4511-Å line is predominantly observed in emission rather than in absorption. Such a behaviour was explained by excitation of fluorescence from the upper ^2S

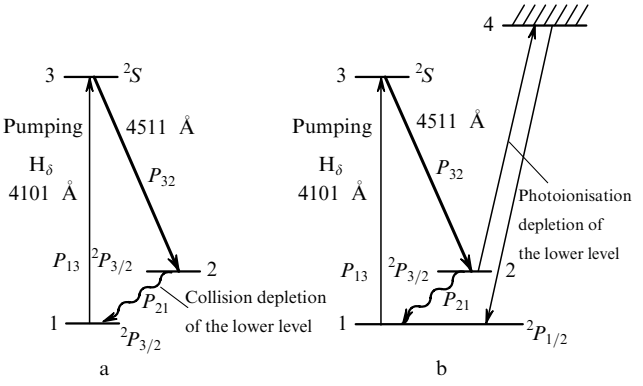

Figure 4. Schemes of cyclic transitions in In I considered in Ref. [8] for explaining the bright emission line at 4511 Å observed upon excitation by the 4101-Å H_δ line: (a) collision and (b) photoionisation depletion of the metastable $^2P_{3/2}$ level (2).

level because of the coincidence of the resonance absorption line of In I at 4101.72 Å with a strong emission H_δ line at 4101.75 Å.

Fig. 4a shows the scheme of transitions between three lower levels of In I upon excitation of fluorescence from level 3, which was considered by Thackerey as early as 1935 [8]. The condition for the appearance of an emission line rather than an absorption line at the $3 \rightarrow 2$ transition found by Thackerey proved to be coincident with the inversion condition. Indeed, let us assume that radiation of intensity I_{13} acts on the resonance transition and radiation of intensity I_{23} acts on the anomalous transition. The $2 \rightarrow 1$ transition is forbidden, and a cyclic transition between states 1, 2 and 3 is impossible in the atom. Because the In atom has a low ionisation potential (5.76 eV), it is reasonable to include atoms in state 4 into the scheme. Under the conditions

$$P_{14} = P_{24}, \quad P_{42} = 2P_{41}, \quad P_{32} = 2P_{31}, \tag{1}$$

for the transition probabilities, which take into account the degeneration of the levels and the fact that levels 1 and 2 are the states of the same term, we obtain the following expression for level populations n_i in a stationary state:

$$n_1 \frac{P_{23}}{P_{23} + P_{24}} = n_2 \frac{P_{23}}{2(P_{23} + P_{24})}$$

$$= n_3 P_{32} \left[2P_{13} + \frac{4}{3} P_{24} + \frac{2}{3} P_{13} \frac{P_{24}}{P_{23}} \right]^{-1}. \tag{2}$$

Therefore, the ratio of the numbers of emission ($3 \rightarrow 2$) and absorption ($2 \rightarrow 3$) transitions at the frequency ν_{23} is [8]

$$\alpha = \frac{n_3 P_{32}}{n_2 P_{23}} = 1 + \frac{P_{24}(P_{13} - P_{23})}{3(P_{13} + P_{24})}. \tag{3}$$

For $\alpha > 1$, the cyclic $1 \rightarrow 3 \rightarrow 2 \rightarrow 4 \rightarrow 1$ transition occurs, resulting in the predominant emission at the $3 \rightarrow 2$ transition.

Note that the condition of the cyclic transition $\alpha > 1$ in the $3 \rightarrow 2$ direction is simultaneously the population inversion condition for levels 2 and 3:

$$\alpha = \frac{n_3 P_{32}}{n_2 P_{23}} = \frac{n_3 \sigma_{32}}{n_2 \sigma_{23}} = \frac{n_3}{g_3} \Big/ \frac{n_2}{g_2} > 1, \tag{4}$$

where σ_{km} is the cross section for the radiative $k \rightarrow m$ transition. Therefore, the mechanism of amplification of radiation due to stimulated emission has long been used implicitly in the theory of stellar spectra for the description of the so-called emission lines. The fluorescence mechanism of excitation [6] (Fig. 3) is in fact the astrophysical analogue of a three-level scheme with optical pumping [30, 31]. Astrophysicists have proposed the schemes to explain anomalies in stellar spectra, which anticipated a number of laser schemes. For example, Fig. 4b shows the scheme of transitions between the lower levels of In I, which was also proposed by Thackerey [8] to explain the 4511-Å emission line. The cyclic $1 \rightarrow 3 \rightarrow 2 \rightarrow 1$ transition in this scheme and, hence, the population inversion for states 3 and 2 are achieved due to fast collision relaxation of metastable level 2. This scheme is very close to the scheme of a collision laser proposed by Gould [19].

Stimulated emission lines should be narrower than spontaneous emission lines. The narrowing of the spectrum can be quite sufficient for the unambiguous determination of the origin of the emission line. This problem should be considered in more detail, taking into account the existence of a great optical thickness for the amplifying transition and resonance scattering of radiation. In principle, two operating regimes are possible: the amplification of the photosphere emission and amplification of the spontaneous emission of the atmosphere. In the first case, we deal with a narrow-band nonlinear laser amplifier of an external broadband signal, and in the second case, with a resonance laser amplifier of a spontaneous noise. In the latter case, the laser amplifier can be easily transformed to an oscillator due to an inevitable scattering of radiation if the rate of radiation returning to an amplifying region due to scattering exceeds the rate of radiation escape to the environment. Then, resonance scattering results in the appearance of incoherent energy feedback in the amplifying medium [32, 33]. This effect should divide the amplifying region into many separate regions, with lasing thresholds achieved in each of them. The effect of incoherent feedback in the astrophysical laser is considered in more detail in Refs [34, 35] (see Section 8).

4. How is laser action manifested under astrophysical conditions?

After the discovery of microwave space masers operating on the OH radical [4] and H_2O molecule [5], masers operating on more than one hundred molecules were discovered [36], as well as masers operating on highly excited hydrogen atoms in the millimetre region [37]. Stimulated emission of the CO_2 molecule in the IR spectral region at 10 μm was discovered in the atmospheres of Mars and Venus [38, 39]. The characteristic feature of laser action is a high brightness of emission of laboratory lasers, a high brightness of emission also being inherent in astrophysical masers operating on microwave transitions in molecules. Because the brightness temperature of astrophysical masers is extremely high ($10^{12} - 10^{18}$ K) [36], one can make an erroneous conclusion about 'laser action' by observing the anomalous high intensity and the anomalous intensity ratio even in the absence of inversion due to an inappropriate relation between the lifetimes of the quantum levels involved in the 'laser' transition [40]. In this case, another, sometimes rather nontrivial explanation of the anomalous high intensity [41] and the anomalous intensity ratio for spectral lines [42], should be proposed.

Let us explain the 'mistake' about a high brightness of laser lines under astrophysical conditions by comparing the astrophysical microwave maser with the astrophysical optical laser pumped due to an accident coincidence of spectral lines (the Bowen mechanism) [6]. First recall the origin of an extremely high brightness of laser emission. Although this explanation is trivial, it is descriptive and useful for comparison of laboratory and astrophysical lasers.

The active medium of a laser emits a great portion of energy, both below and above the threshold, isotropically and spontaneously in all spatial modes. Even well above the threshold, the fraction of isotropic spontaneous emission remains comparable with that of stimulated emission (Fig. 5a). Above the lasing threshold, the upper-level

population remains invariable at the threshold level (continuous regime), while the total above-threshold pump energy is spent for stimulated emission, which is emitted, however, in a limited (especially over the angle) number of modes. For this reason, the intensity of the directional emission, i.e., of the laser beam greatly exceeds that of the spontaneous emission within this small solid angle (Fig. 5b). Therefore, the high intensity of laser emission is explained by its low divergence and a small observation angle (only along the direction of the laser beam propagation). Under astrophysical conditions, the situation is completely different. Because even incompletely isotropic stimulated radiation of the APL is emitted within a large solid angle (even in the case of the scattering feedback, see Section 7), it should not be anomalously bright against the background of spontaneous emission.

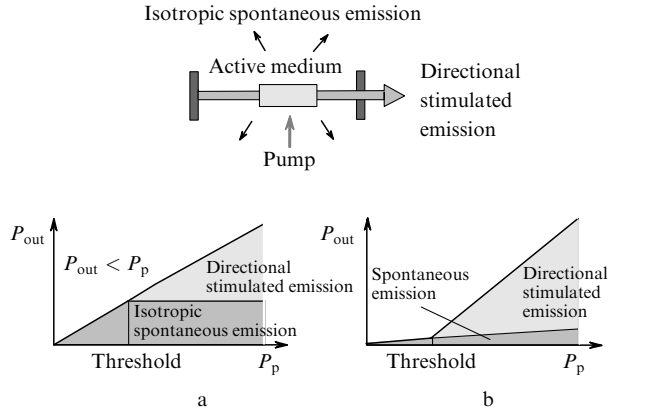

Figure 5. Spontaneous and stimulated laser emission, integrated over the direction of a total emitted power (a) and over the power of directional radiation (b).

This brings up the question: Why is emission of the astrophysical maser in the microwave range so anomalously bright? The reason for this is completely different and is not discussed usually. Fig. 6 shows schematically the origin of emission of a gaseous space cloud without and with inversion at the microwave transition frequency ω_{21}.

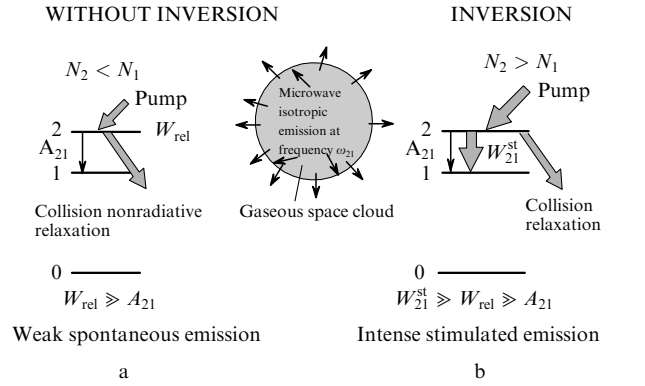

Figure 6. Isotropic microwave emission of a gaseous space cloud without inversion (a) and with inversion at the $2 \rightarrow 1$ transition (b). The pump power in the absence of inversion is spent in the unobservable relaxation channel. In the presence of inversion, the pump power is transformed to the observed intense stimulated microwave emission.

In the absence of the population inversion, a very weak spontaneous microwave emission is observed because the Einstein coefficient is extremely small in the microwave region ($A_{21} = 10^{-7} - 10^{-9}$ s^{-1}), corresponding to the spontaneous emission lifetime from 0.3 to 10 years (!). Of course, collisions occur more often even in a rarefied stellar medium, and even this weak spontaneous emission is suppressed in collisions and a greater part of the pump energy degrades over a nonradiative channel, i.e., an observer does not detect it. If the pump is intense enough to provide the population inversion at the $2 \rightarrow 1$ transition, and the size L of the gaseous cloud provides the gain factor $\alpha L \gg 1$ that ensures a considerable gain ($K = \exp \alpha L \simeq 10^{10} - 10^{15}$), stimulated emission develops. Because the rate W_{21}^{st} of stimulated transitions can become equal to the rate of collision (unobserved) relaxation and even exceed it, almost all the pump energy is spent for stimulated emission being observed, which can have an enormous brightness temperature. In other words, due to the maser effect, a weak spontaneous emission line, which is not observed in radio astronomy, is transformed to a strong stimulated emission line acquiring energy from the unobserved channel. Therefore, the astrophysical maser has a high brightness because it is not pumped by another microwave radiation, which is very weak.

A completely different situation takes place for the APL in the optical spectral region (Fig. 7). Let us assume that level 3 is optically excited by a spectral line of another element (directly or via a high-lying state relaxing to state 3). In the absence of population inversion in the system of three levels (1, 2, 3), we observe, for example, a pair of spontaneous emission lines, with the intensity ratio equal to the ratio of the Einstein coefficients A_{32} and A_{31}. We assume for clarity that the $3 \rightarrow 2$ transition in Fig. 7 is very weak ($A_{32} \ll A_{31}$) and, hence, almost all energy of particles excited to level 3 relaxes due to the $3 \rightarrow 1$ spontaneous emission at the frequency ω_{31}, whose intensity is virtually equal to that of the line pumping level 3.

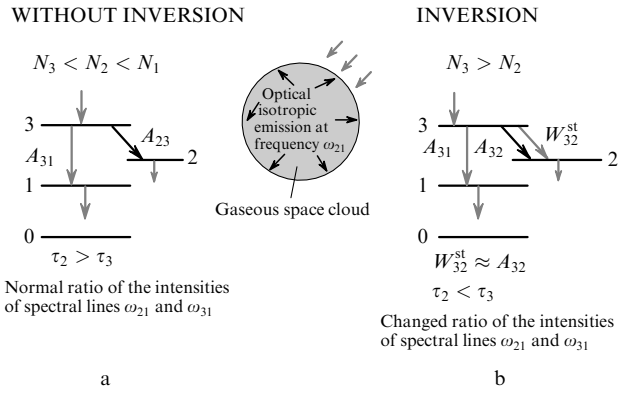

Figure 7. Passage from spontaneous isotropic emission in a medium without inversion (a) to spontaneous isotropic and stimulated isotropic emission in a medium with inversion (b).

Assume now that the spontaneous decay time τ_3 of level 2, to which particles from level 3 undergo transitions comparatively rarely, is much shorter than $1/A_{12}$, so that the population inversion always exists for the $3 \rightarrow 2$ transition. Then, the $3 \rightarrow 2$ transition becomes amplifying, and the gain may exceed the ratio of the spontaneous decay

rates A_{31}/A_{32} when the size of the amplifying region is sufficient. In this case, the stimulated transition rate W_{32}^{st} can become not only equal to the spontaneous decay rate A_{31} but also exceed it. The main relaxation channel of particles at the level 3 is stimulated emission at the frequency ω_{32}. In this case, the intensity of the weak $3 \rightarrow 2$ transition increases and achieves that of the line pumping level 3 (but does not exceed it).

In other words, the laser line of stimulated emission cannot be brighter than a spontaneous line exciting level 3. For this reason, the criterion of the anomalous intensity of the laser line compared to other bright pumping spectral lines cannot be used for the search for laser lines. This circumstance substantially differs from the case of masers, when the pump intensity is not related to microwave emission and, therefore, can be quite high. The conversion of the excitation energy to stimulated microwave emission makes the latter anomalously bright. It is clear from these simple qualitative reasoning that laser action should be manifested in the increase in the intensity of very weak spontaneous emission lines up to the intensities of spontaneous emission lines at allowed transitions, i.e., the transitions with small Einstein coefficients ($A_{32} \simeq 1 - 10^5$ s^{-1}).

Note that the above discussion concerns the optical pump of APLs, which seems to be the most probable for the optical range. It is not inconceivable that other pumping methods exist, which are based on collisions. However, one should bear in mind that the spontaneous relaxation rate even for metastable levels is very high compared to that in the microwave range. This makes the possibility of collision pump producing the population inversion less probable than purely optical excitation because of the coincidence of the emission and absorption lines of two different particles.

5. Fe II astrophysical laser in the region of gas condensation near a hot star

The vicinity of a bright star is a unique place where hydrogen atoms (of the most abundant element of the Universe) are photoionised under the conditions of high vacuum by the VUV radiation from the star (Lyman emission continuum at $\lambda < \lambda_c = 912$ Å). Free protons and electrons being formed upon photoionisation recombine in subsequent rare collisions by emitting characteristic spectral lines of H I, 70 % of the energy being emitted in the 1215-Å Ly$_\alpha$ line. This spectral line is not observed at the Earth because of absorption by the interstellar hydrogen at an extremely low concentration. However, a substantial role of the intense Ly$_\alpha$ line is manifested in the effects produced by this emission, in particular, upon resonance photoexcitation of atoms and ions of other, more rare elements. It is for this reason that laser action is observed in the region of a compact gas condensation in the vicinity of the η Car star [18].

The possibility to use resonance optical excitation for pumping one chemical element by radiation from another chemical element for producing the population inversion and creating a laboratory optical laser was considered already in the first paper where the laser was proposed [43]. Such a coincidence of spectral lines is a quite rare phenomenon because of a small width of the spectral lines of free atoms and ions, and it is not virtually used in modern lasers. However, this phenomenon is at the basis of the mechanism of formation of some spectral lines of nebulae, which represent mixtures of many atoms and ions irradiated by intense spectral lines of hydrogen or helium [6]. The possibility of laser action due to this mechanism was also considered long ago [17], but this effect is difficult to observe against the background of the intense emission of the star photosphere.

The situation changed drastically after the creation of the Hubble Space Telescope (HST) in combination with the Space Telescope Imaging Spectrograph (STIS), which provides a high spectral and angular ($\sim 0.1''$) resolution in a broad spectral range from 1150 to 10400 Å [44]. Beginning from 1998, the eruptive η Car star became a remarkable observation object [45]. This star is an exclusively interesting astronomic object, which ejects a huge amount of a stellar matter to the environment during many explosions. In particular, after a powerful explosion in 1840, this star was the second in the brightness at the vault of heaven in the South hemisphere. The ejected matter formed the huge ($8'' \times 16''$) environment of the star, which was called Homunculus. This very inhomogeneous and structured nebula is a remarkable object of our Galaxy. In particular, compact gas condensations (GCs) emitting very bright Fe II lines were discovered in the nearest vicinity of the central star at a distance $R_b = 100 - 1000$ radii of its photosphere [46]. These condensations are also unique astrophysical objects because the concentration of hydrogen in them ($N_H = 10^7 - 10^{10}$ cm^{-3}) [47] is much higher than that in a typical planetary nebula (10^4 cm^{-3}) and they are located at a distance of only a few light days from the central star.

Because of a relatively high local concentration of hydrogen in GCs, the Lyman continuum emission of the η Car star is almost completely absorbed by them. In other words, the Stromgren boundary [48] separating the region of completely ionised hydrogen from the region of neutral hydrogen passes inside the GC, as shown schematically in Fig. 8, i.e., a completely ionised front part of the GC (the H II region) is directly adjacent to the neutral H I region. The spectral intensity of Ly$_\alpha$ emission generated in the H II region due to the photoionisation-recombination cycle is $10^3 - 10^4$ times greater than the intensity of a weakened Ly$_\alpha$ emission coming from the central star. This occurs due to a substantial compensation of the effect of weakening of the star emission owing to a narrow-band Ly$_\alpha$ emission formed upon absorption of a broadband Lyman continuum and, to

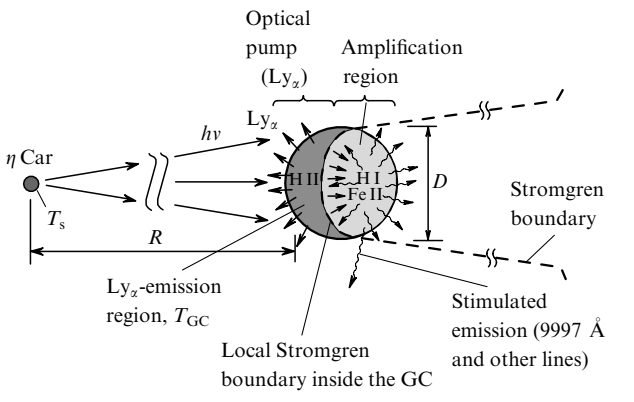

Figure 8. Photophysical model of a compact gas condensation (GC) near the hot bright η Car star with the local Stromgren boundary between the photoionised (H II) and neutral (H I) regions inside the GC [18].

some extent, because of trapping of Ly_α emission in the optically thick (for Ly_α emission) H II medium. As result, a unique situation takes place, when a weakly ionised mixture of many readily ionised atoms in the neutral H I region is exposed to radiation with a high spectral intensity at the Ly_α wavelength coming from the adjacent completely ionised region. (This resembles a typical 'laser' situation, when a flashlamp irradiates the adjacent active laser medium!) At the same time, a high angular resolution of the HST/STIS allows the observation of the emission spectra of GCs separately from the bright emission of the photosphere of the central η Car star [49].

Because of the high density of hydrogen, the Lyman emission continuum ($\lambda < 912$ Å) is completely absorbed in the front part of the GC due to photoionisation of hydrogen (Fig. 8) and approximately 70 % of this radiation is emitted at 1215 Å upon recombination (the Lyman α line). This monochromatic radiation is strongly broadened during radiation transfer in the optically dense neutral H I region of the GC and is capable of exciting a number of quantum transitions in the Fe II ion in the unionised (rear) part of the GC, as shown in Fig. 8. The Fe II ions are produced upon photoionisation of Fe at a concentration of about $10^{-4}N_H$ by the star emission in the region $\lambda > 912$ Å. This emission readily propagates through the photoionised front part of the GC.

The spectrum of Fe II is rich in quantum transitions. The density of the absorption lines of Fe II in the Ly_α region is of about 15 lines per 1 Å. Upon diffusion of the Ly_α emission in the resonantly scattering H I region with a high optical density, the spectral lines are strongly broadened (up to a few hundreds cm^{-1}). Due to such broadening, the Fe II ions are optically excited to high quantum levels [50]. This is manifested in the appearance of the fluorescence lines of Fe II, which can be rather bright, as for example, the UV fluorescence lines of Fe II (at 2507 and 2509 Å) [51]. Fig. 9a shows the scheme of excitation of the $1 \rightarrow 4$ transition in Fe II by the 1215.671-Å Ly_α emission line [18]. The frequency detuning $\Delta\nu$ is only 30 cm^{-1} and is compensated by a strong broadening of the Ly_α line (up to 300 cm^{-1}) during radiation transfer. Stage 4 decays predominantly due to radiative transitions to state 3, which has a rather small Einstein coefficient ($A_{21} \simeq 8 \times 10^4$ s^{-1}). Because level 2 (Fig. 9a) decays very rapidly, the population inversion always exists at the $3 \rightarrow 2$ transition, so that level 3 is a 'bottleneck' of radiative relaxation of the highly excited Fe II.

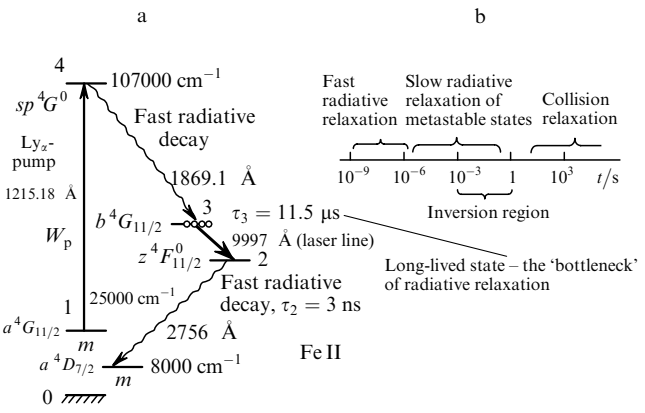

Figure 9. Producing the population inversion at the $3 \rightarrow 2$ transition in Fe II upon resonance excitation of the high-lying level 4 followed by the cascade radiative decay to the long-lived 'pseudo-metastable' level. (a) Scheme of the population inversion and transitions and (b) characteristic times of the radiative and collision relaxation of the excited levels of Fe II [18].

Let us make simple estimates of the gain α_{23} using the model [41] of photoprocesses in the GC in the near vicinity of the η Car star. The rate of photoselective excitation of the state 4 is determined by the expression

$$W_p^{14} = A_{41}\left[\exp\left(\frac{h\nu_{14}}{T_{GC}}\right) - 1\right]^{-1}, \tag{5}$$

where $A_{41} = 1.2 \times 10^7$ s^{-1} is the Einstein coefficient for the spontaneous decay of state 4 to state 1 and T_{GC} is the brightness temperature of the Ly_α emission inside the GC. For $kT_{GC} \simeq 1.0 - 1.5$ eV $[T_{GC} \simeq (12 - 18) \times 10^3$ K], the excitation rate is $W_p^{14} \simeq 10^3 - 10^4$ s^{-1}.

The main decay channel (97 %) of the state 4 is the radiative transition to two levels of the $b\,^4G$ fine structure. One of the levels (the $b\,^4G_{11/2}$ level of state 3) decays spontaneously with emission with the probability $A_{32} = 8 \times 10^4$ s^{-1} to state 2 ($z\,^4F^0_{9/2}$) with a short lifetime (~ 3 ns). It is at the $3 \rightarrow 2$ transition that the stationary population inversion appears with the density ΔN:

$$\Delta N = N_3 - N_2 = N_3 = (W_p^{14}\tau_3)N_1, \tag{6}$$

where $N_2 \ll N_3$ because of the fast decay of level 2; $\tau_3 = 11.5$ μs; N_1 is the population density of the initial metastable level with the lifetime $\tau_1 \simeq 0.77$ s $\gg \tau_3$.

The linear gain on the $3 \rightarrow 2$ transition (9997 Å) is determined by a standard expression

$$\alpha_{32} = \sigma_{32}\Delta N, \tag{7}$$

where ΔN is the inverted population density determined by expression (6). The cross section σ_{32} for the stimulated transition is described by the expression

$$\sigma_{32} = \frac{\lambda_{32}^2}{2\pi}\frac{A_{32}}{2\pi\Delta\nu_D}, \tag{8}$$

where $\Delta\nu_D$ is the Doppler width of the $3 \rightarrow 2$ transition in Fe II. At the temperature of a relatively cold H I region equal to 100 – 1000 K, the width is $\Delta\nu_D \simeq 300 - 1000$ MHz, i.e., $\sigma_{32} \simeq (0.6 - 2) \times 10^{-13}$ cm^2. Therefore, the gain can be estimated from the expression

$$\alpha_{32} = \sigma_{32}(W_p^{14}\tau_3)fN_0, \tag{9}$$

where f is the fraction of Fe II ions in the initial metastable state with respect to the rest of the states of Fe II (all the Fe I atoms are photoionised in the H I region).

The fraction f of ions is determined by the rate of excitation of level 1 and its decay time. The rates of collision mechanisms of excitation of level 1 (i.e., the recombination of Fe^{2+} ions and collisions of Fe^+ with electrons) are

negligible compared to the decay rate $1/\tau_1$ because the electron concentration in the H I region is low ($n_e \simeq 10^4 - 10^5$ см$^{-3}$) due to photoionisation of the atoms of iron and other elements with the ionisation potential $I < 13.6$ eV.

The level 1 is predominantly populated due to optical excitation of other transitions by a broad Ly_α band. These transitions occur from the lowest, more populated metastable levels (with energy ~ 1 eV). After the decay of the excited levels, low-lowing metastable and pseudo-metastable levels with higher energies (2–3 eV) are populated. These excitation channels can provide the excitation rate of level 1 of the order of $1/\tau_1 \simeq 1\ s^{-1}$, thereby maintaining the relative population f of state 1 equal, for example, to $\sim 10^{-2}$. This corresponds approximately to the uniform distribution of Fe II ions among 90 metastable and pseudo-metastable states, including state 1. The validity of this estimate is confirmed by the observation of intense fluorescence lines of Fe II at 2507 and 2509 Å [51], which appear upon selective excitation by the Ly_α line of the transition whose lower level $a^4D_{7/2}$ has the energy 0.99 eV.

According to (9), within the framework of these assumptions, the linear gain at the $3 \to 2$ transition is $\alpha_{32} \simeq (3 \times 10^{-18} - 10^{-16})N_0$, where $N_0 \simeq 10^{-4}N_H$ is the density of iron atoms transformed to Fe II. According to the data [41] and calculations of the critical density of hydrogen atoms in the GC [41], the concentration of N_H in the GC is obviously higher than 10^8 cm^{-3}. Therefore, for $\alpha > (3 \times 10^{-14} - 10^{-12})$ cm^{-1} and the GC size $D \simeq 10^{15}$ [47], which can be taken as the size of the amplifying region (see Fig. 8), we have $\alpha L \simeq 30 - 1000$ for the brightness temperature of the Ly_α line in the GC $T_{GC} = (12 - 18) \times 10^3$ K.

This corresponds to rather high values of the linear gain $K = \exp(\alpha_{32}L)$. However, for $K \simeq A_{43}/A_{42} \simeq 10^3$, the intensity of isotropic radiation in a weak λ_{32} line approaches the intensity of the λ_{43} line, which provides excitation of level 3, i.e., the pumping is depleted. In other words, the amplification regime is saturated, and the intensity of the weak λ_{32} line becomes comparable with that of the λ_{43} line, i.e., its intensity (measured in photon cm^{-2} s^{-1}) increases by a factor of $A_{43}/A_{32} \simeq 10^3$. It is this effect that was observed for a number of weak lines of Fe II [49, 52].

Laser amplification and stimulated emission in the optical region are probably quite common processes in gaseous media in the vicinity of bright stars. They appear due to the features of the relaxation of excitation of the electronic levels of atoms (ions) in a rarefied circumstellar and interstellar gas. Relaxation processes have different characteristic times (see Fig. 9b). The radiative relaxation caused by spontaneous emission occurs for $10^{-9} - 10^{-3}$ s (sometimes even for $10^{-3} - 1$ s), whereas the collision relaxation lasts more than 100 s (for the gas density lower than 10^9 cm^{-3}). In the case of selective excitation of an atom (ion) with a complicated energy level diagram, the radiative spontaneous relaxation in an isolated atom (ion) occurs only due to radiative transitions, without any collisions, producing the population inversion for some pair of levels because of the 'bottleneck' effect. If the GC size is sufficient to obtain a substantial gain at the inverted transition, then a faster relaxation, caused by stimulated emission, begins. Therefore, the laser action provides the radiative cooling caused by stimulated emission of GC at inverted transitions along with spontaneous emission at conventional transitions without the population inversion.

6. Oxygen atom astrophysical laser

We have mentioned in Section 3 the anomaly in the behaviour of the 8446-Å and the 7774-Å lines in the spectra of the Be stars [23, 25], which was later naturally explained by stimulated emission at the inverted transition at 8446 Å [17] upon pumping the upper level by the bright 1025.72-Å Ly_β line of H I according to the Bowen scheme [26] shown in Fig. 3a. Moreover, Bennett *et al.* [53] obtained cw lasing at 8446 Å in a laboratory. The population inversion was achieved in an electric discharge in a mixture of oxygen and noble gas at a low pressure. Similar conditions can exist in stellar atmospheres. The normal intensity of the 7774-Å line can be naturally explained by the laser action. Indeed, the lower level of the transition corresponding to this line is metastable, and no inversion and gain can be produced at this transition. The appearance of the population inversion and the gain at the $3p\,^3P \to 3s\,^5S$ transition in O I in atmospheres of the Be stars was analysed in detail in paper [34].

One can see that the scheme of transitions in Fig. 3a coincides with the scheme of a four-level generator and that, due to a favourable relation between the probabilities A_{ij} of the $3 \to 2$ and $2 \to 1$ spontaneous transitions (the probabilities of spontaneous transitions calculated by the method [54] and the degeneration multiplicity of the levels are: $A_{21} \simeq 5 \times 10^8\ s^{-1}$, $A_{32} \simeq A_{43} \simeq A_{41} \simeq A_{4'1'} \simeq A_{3'2'} \simeq 3 \times 10^7\ s^{-1}$, $A_{2'1'} = 10^5\ s^{-1}$, $A_{4'3'} = 2 \times 10^6\ s^{-1}$; $g_1 = 9$, $g_2 = 3$, $g_3 = 9$, $g_4 = 15$), the population inversion can be produced at the $3 \to 2$ transition.

Consider a gas consisting of oxygen atoms with the density N_0 and temperature T_0 in the radiation field with the spectral density U and frequency $\omega \approx \omega_{41}$. The balance equations for population in the stationary case are presented in [34]. It is known that the pump threshold in four-level lasers is substantially determined by the population of level 2, which depends on the temperature of radiation acting at the $1 \to 2$ transition (in the case under study, the contribution of nonradiative transition is small). If the gas were in equilibrium with radiation, the radiation temperature would be coincident with the gas temperature T_0. However, a more hot radiation is present in stellar regions, which is emitted by the photosphere and has the temperature T, which noticeably exceeds T_0.

The density of O I atoms in the atmosphere region located near the external boundary of the photosphere (in the inverting layer) is $N_0 \sim 10^5 - 10^6$ cm^{-3}, the gas temperature here is $T_0 \sim 1.5 \times 10^4$ K, and the effective temperature of the photosphere is $T_* \sim 3 \times 10^4$ K [55, 56]. If we assume that the radiation temperature at the $1 \to 2$ transition is $\sim T_*$, then, as follows from analysis [34], the required brightness temperature of pump radiation at the threshold should be 4×10^4 K, while to obtain the population inversion, for example, $\Delta N_{32} \sim 10^{-6}N_0$, this temperature should be greater ($\sim 4.1 \times 10^4$ K).

Except optical pump, the contribution from collisions with electrons into the population inversion at levels 2 and 3 (excitation of level 3 through the metastable level in Fig. 3a) was also estimated. No inversion is obtained upon excitation of the $1 \to 2$ transition by radiation with the temperature T* in the absence of radiation at other transitions.

We can estimate now the possible value of the gain α for the 8446-Å line of O I in the atmosphere of the Be star. For $A_{32} = 3 \times 10^7\ s^{-1}$ and $\Delta\omega_D \simeq 5 \times 10^{10}\ s^{-1}$, the cross section for the $3 \to 2$ radiative transition is, according to (8),

$\sigma_{32} \simeq 10^{-12}$ cm^2. For $\Delta N_{32} \simeq 1$ cm^{-3}, this corresponds to the gain at the line centre $\alpha_{32} \simeq 10^{-12}$ cm^{-1}. Taking into account that the extension of the atmosphere of the Be stars is $10^{13} - 10^{14}$ cm [55, 56], we can conclude that the inverted population with the linear gain factor $\alpha L \simeq 10 - 100$ appears in the stellar atmosphere.

Note the possibility of optical excitation of the photosphere by continuous radiation without the resonance coincidence. To obtain the population inversion in this case at some transition, the spectrum of continuous radiation should be nonequilibrium. Mustel' [57] has shown that the continuous spectrum of the photosphere can strongly differ from the Planck distribution. Although in the case of O I under study, the radiation spectrum is not nonequilibrium enough for producing the population inversion at the $3 \rightarrow 2$ transition, the nonequilibrium distribution of radiation should be taken into account in the calculation of other astrophysical situations when the gaseous circumstellar medium is found in spatially and radiatively inhomogeneous conditions. Note among them first of all the symbiotic stars, in which the short-wavelength emission from a hot star irradiates the atmosphere of a colder star. Under such conditions, laser action can be observed for many atoms and ions.

Another potential region for the appearance of the population inversion and gain, in particular, for the 8446-Å O I line is the Stromgren boundary region, which separates the ionised H II medium from the almost neutral H I medium. In this boundary region, the bright Ly_β line of the H I region, generated to the H II region, irradiates the H I region, where oxygen is in the neutral state because the photoionisation limit for the 8446-Å O I line ($I_{OI} =$ 13.618 eV) lies above the Lyman emission continuum limit (13.5985 eV). Under such conditions, the Ly_β line should efficiently excite neutral oxygen namely in a comparatively thin Stromgren boundary region. Therefore, it is quite probable that a strange behaviour of the 8446-Å O I line in the Orion Nebula observed in paper [58] can be attributed to laser action. The authors of this paper discovered a unique intense structure in the intermediate H II/H I region only by observing the very intense 8446-Å line. At other lines of O I and at the H_α Balmer line (which should be present in the regions of the intense Ly_β line), radiation has a spatially amorphous stricture, without any filaments.

The authors of paper [58] explained this unique fact by assuming the existence of solid particles in this intermediate region, which affect in some way the morphology and the emission spectrum of O I, and pointed out the necessity of a further study of this strange situation. High-resolution spectroscopic measurements with the use of a Fabry–Perot interferometer [58] showed that the width of the 8446-Å line was approximately narrower by 25 % than that of the 6300-Å line. It seems to me that all these observations can be more naturally explained assuming the gain at the 8446-Å transition, where the population inversion should be certainly exist. Of special attention is a remarkable fact that a point (unidentified) radiation source ('emitting object' [59]) is observed in the Orion Nebula, which is not observed at the 8446-Å line (!). This suggests that the radiation pattern of the amplifying region can be anisotropic, with a maximum that is not directed to an observer. This possibility should be specially studied with the help of the HTS/STIS.

7. Radiation pattern and the emission spectrum of an amplifying region

In the absence of a feedback (see Section 8), the amplifying medium of the astrophysical laser represents a spontaneous emission amplifier. This type of the laser device in most common in the VUV and X-ray quantum electronics, where it is difficult to produce the cavity feedback because of the short amplification time and (or) the propagation of the amplification region together with a pump pulse. Because of the large size of the astrophysical amplification region, the condition

$$\frac{a}{L} \gg \frac{\lambda}{a} \tag{10}$$

is always fulfilled, where a and L are the transverse and longitudinal sizes of the amplification region, so that the radiation pattern is determined by the geometry of the amplifying region. In the case of a nearly spherical geometry ($a \simeq L$), the radiation should be isotropic. This statement concerns, strictly speaking, a linear amplification regime. In the saturated amplification regime, a small deviation from sphericity should be distinctly manifested, and we can assume, based on heuristic considerations, the existence of a peculiar instability of the spherical geometry of radiation from a saturated amplifier. However, this question calls for separate investigation. Because the probability of formation of spherical amplification regions even in boundary astrophysical regions, where the appearance of the population inversion is most probable, is very low (although is not zero), it is most likely that the formation of the anisotropic patterns of stimulated emission will depend on the geometry of the amplification regions, although it is unlikely that the directivity of these patterns will be high. The latter remark is essential for the qualitative explanation of the emission spectrum of a saturated amplifier when the gain line is inhomogeneously broadened due to the Doppler effect.

In the regime of linear amplification of spontaneous emission, the width of its spectrum decreases because of a predominant amplification of emission at the line centre, which is described by a simple law [60–63]

$$I = \frac{I_0(v)}{(1 + \alpha L)^{1/2}}, \tag{11}$$

where α is the gain coefficient per unit length (cm^{-1}). This occurs until the saturation of the inhomogeneously broadened gain line is accompanied by the 'flattening' of its peak. This effect was considered for the astrophysical laser saturated amplifier and it was shown [62] that the narrowing of the spectrum ceases upon saturation and the spectrum broadens again up to the width of the gain line, as is demonstrated qualitatively in Fig. 10. This conclusion was confirmed by many experimental data for astrophysical masers [1, 64–66] with the only exception. In paper [66], an anomalously narrow emission spectrum of the 18.5-cm OH maser was observed, whose width corresponded to the Doppler width at the temperature $T \simeq 5$ K. This phenomenon is not explained so far. It was pointed out in Ref. [35] that the conclusion of paper [62] is valid only for directional emission, when the saturation of the Doppler profile is accompanied by flattening of its peak. In reality, the satu-

ration of the Doppler profile under the action of isotropic radiation is not accompanied by its deformation but occurs uniformly [68] (Fig. 11), while the narrowing of the isotropic radiation line is not followed by its broadening and should obey the law (11). This probably explains the anomalously narrow width of the emission spectrum of the OH maser [67]. The fact that this case is quite rare confirms the conclusion that the nearly spherical geometry of the amplifying region is also encountered rarely.

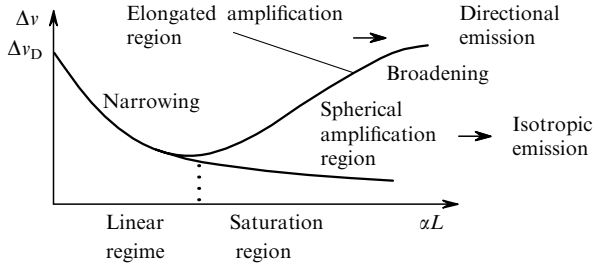

Figure 10. Evolution of the width of the spontaneous emission spectrum in a saturated amplifier at the Doppler transition for a spherically isotropic amplifier and directional emission of an elongated amplifier.

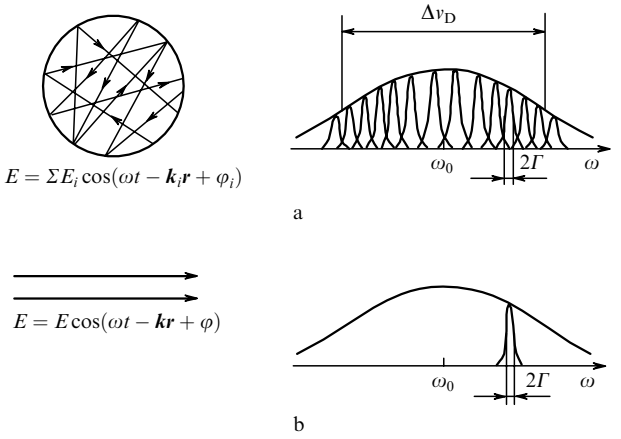

Figure 11. Interaction of monochromatic isotropic (a) and directional (b) emission with a Doppler profile. Because isotropic emission does not burn a hole in the profile, the entire Doppler profile is saturated, without any deformations [68].

The resolving power of both ground and space spectrometers in the optical range does not exceed $R = \nu/\Delta\nu \simeq 2 \times 10^5$, i.e., it is of the order of the Doppler width of spectral lines emitted from regions with kinetic temperatures lower than 10 000 K. For this reason, unlike the astrophysical maser, the experimental possibilities for investigations of APLs are very limited at present (see Section 9).

8. Feedback due to scattering in the APL

In quantum electronics, a positive feedback with the help of a Fabry–Perot resonator or its modifications is commonly used [43, 69] (Fig. 12a). An open optical resonator performs in fact two functions: the returning of a certain fraction of radiation energy emitted by the active medium back to the medium and the formation of a rather small number (compared to a huge number in the volume $V \gg \lambda^3$) of stable configurations of the electromagnetic field due to the constructive interference of incident and reflected waves in the resonator elements. Therefore, the positive energy and phase feedback takes place.

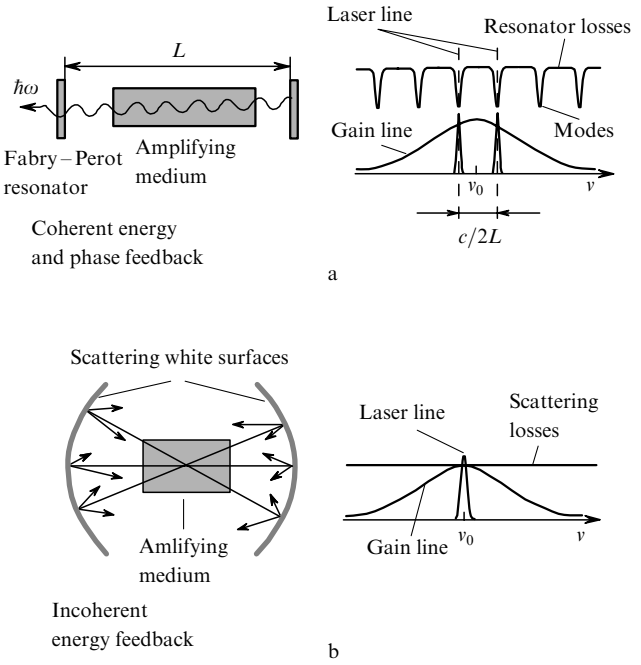

Figure 12. Coherent phase and energy feedback provided by an open Fabry–Perot resonator (a) and incoherent energy feedback produced by scattering reflectors (b).

However, the positive feedback can be also effective only over the energy but not over the phase, i.e., without the establishment of a stable configuration of the electromagnetic field in the active medium and without the formation of a small number of resonance modes. This was demonstrated in experiments supervised by N.G. Basov as early as the mid-1960s [70–72]. In these experiments, a ruby crystal with a high gain per round trip was placed between scattering surfaces (Fig. 12b). When the gain per round trip in the crystal is large enough ($K \gg 1$), even a small fraction of the energy ($\Omega_0/2\pi \ll 1$) returned into the solid angle Ω_0 of the amplifying medium (i.e., when $K(\Omega_0/2\pi) > 1$) is sufficient for lasing. A laser operating in such a regime is called a *nonresonance* (or more exactly *incoherent*) feedback laser. This terminology indicates the absence of the spatial coherence of emitted radiation, which is achieved when the two conditions

$$V \gg \lambda^3, \quad \frac{a}{L} \gg \frac{\lambda}{a} \tag{12}$$

are satisfied, where V and a/L are the volume and the angular aperture of emitted radiation in the amplifying medium, respectively. If conditions (12) are satisfied, a huge number (10^9 and more) of low-Q spatial modes of nearly the same quality lie within even a narrow gain line of the active medium. These modes overlap with each other by producing the frequency-independent (nonresonance) Q-

factor in such a scattering cavity (Fig. 12b). The resonance gain line remains the only resonance element in such a laser, resulting in a slow narrowing of the lasing spectrum to the centre of the gain line [72]. The statistical properties of radiation emitted by such a laser differ, of course, from the properties of coherent light and are close to those of a very bright black-body radiation in a narrow frequency region, as was shown experimentally and theoretically [72].

The idea of a coherent scattering feedback was extended to a more general case of a simultaneously amplifying and scattering medium [73], which also has the lasing threshold, exhibits the narrowing of the emission spectrum, etc, i.e., possesses many characteristics of a laser except the spatial coherence. The radiation statistics of such a scattering laser corresponds to the statistics of equilibrium high-temperature radiation [74]. Many experiments were performed to create scattering dye lasers [75], in particular, an ensemble of microlasers on scattering particles [76]. In the latter case, condition (12) is close to its violation, and therefore fluctuation effects become noticeable upon the interference of a comparatively small number of spatial modes. However, these effects are of no importance in huge astrophysical media.

The possibility of transformation of the astrophysical amplifier to the astrophysical maser using resonance amplification was considered already in Ref. [77], in particular, for amplifying H_2O regions. The experimental data [78] show that this effect can in fact explain the flares of H_2O masers. The role of scattering in the conversion of the APL amplifier to a laser was considered in detail in paper [34].

Here, strictly speaking, we should distinguish three types of scattering: (1) nonresonance scattering by electrons accompanied by a large random Doppler frequency shift, which substantially exceeds the Doppler width of the gain line (Fig. 13a); (2) resonance scattering by amplifying particles themselves accompanied by the random Doppler shift within the gain line width (Fig. 13b); and (3) nonresonance scattering by microparticles whose thermal velocity is much smaller than atomic velocities, so that the Doppler broadening upon scattering is small (Fig. 13a).

The first case is inefficient for producing feedback because of a small fraction of scattered photons returning to the profile of the resonance gain line. The second case is quite suitable for producing feedback, however, the lasing line can narrow down according to (11). In this case, αL is the gain factor per mean free path of a photon until its scattering, because upon scattering the Doppler shift broadens the line again up to the Doppler width. In the third case, the narrowing of the emission line cause by feedback can be quite substantial. The narrowing of the emission line of the scattering feedback APL was calculated in Ref. [34] namely for this case because the Doppler broadening appearing upon scattering was neglected in this paper.

The amplifying and scattering medium has a threshold (critical) radius, at which a fraction of photons leaving the amplifying region due to scattering is exactly compensated by a fraction of photons produced upon amplification [75]. This radius is similar to the critical radius of a neutron reactor, in which neutrons are both multiplied and leave the reactor due to scattering. The critical radius of the scattering feedback APL was calculated in Ref. [34]. For the 8446-Å O I laser in the atmosphere of the Be star, $r_{cr} \simeq 10^{11}$ cm, which is substantially lower than the photosphere diameter for stars of this class. Therefore, many independently operating resonance scattering feedback APLs can appear in the amplification region of a larger size ($L \gg r_{cr}$).

The transformation of the APL amplifier to the APL oscillator affects not only the width of the emission line but also the lasing dynamics. For example, an abrupt change in the pumping rate W_p differently affects the responses of the amplifier and oscillator, as shown qualitatively in Fig. 14. Of course, the characteristic times of these changes are of the order of L/c, which corresponds months under astrophysical conditions to times from a few minutes to a few months. More detailed future observations will probably give the answer to the real role of scattering feedback in APLs and astrophysical masers.

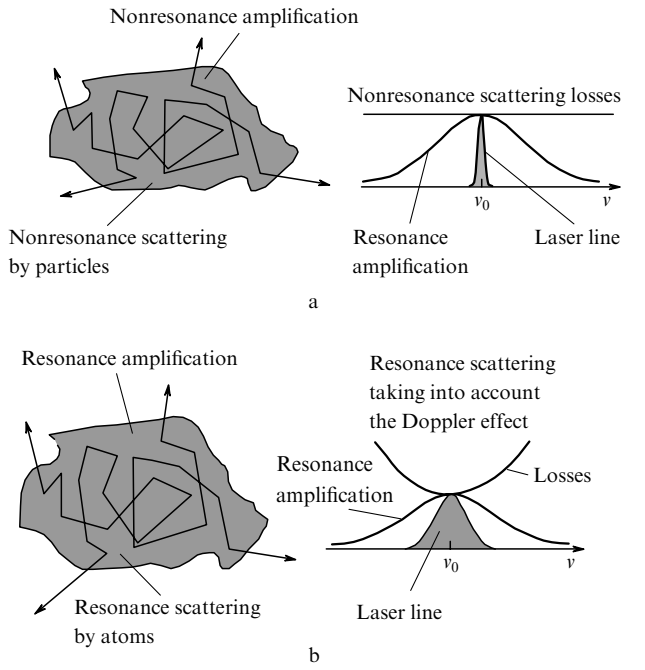

Figure 13. Incoherent feedback produced due to nonresonance (a) and resonance scattering taking into account the Doppler effect (b) caused by moving scattering particles and atoms.

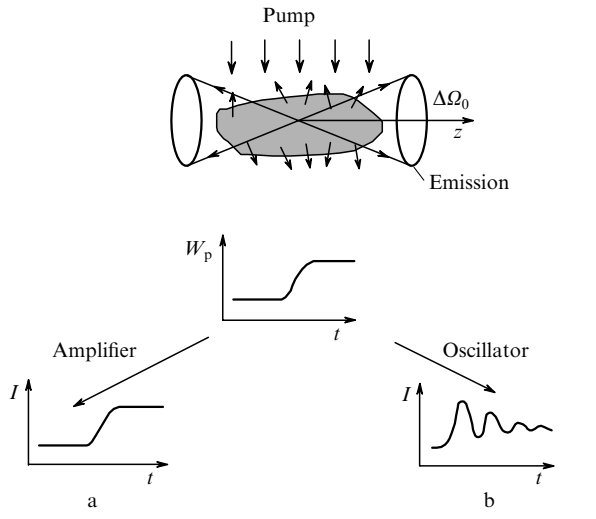

Figure 14. Dynamic response of the amplifier (a) and oscillator (b) to a rapid change in the pump rate.

9. On the observation of lasing under astrophysical conditions

The observation of the narrowing of the emission spectrum would be the best proof of lasing on some spectral lines in stellar atmospheres or in the vicinity of stars. Because the width of the spectrum in this case can be considerably lower than the Doppler width, such measurements can be performed only using high-resolution spectral instruments (for example, a Fabry–Perot etalon). Note also that the narrowing of the emission spectrum can be measured by the correlation method with the help of the Brown–Twiss effect [79, 80], which was described in detail in paper [81] and was also discussed in paper [82].

The statistics of fluctuations in emission of an incoherent feedback laser observed within a narrow solid angle coincides with the statistics of equilibrium (Gaussian) emission, as was shown theoretically and experimentally in Refs. [72–74]. For this reason, by using the correlation method, emission of a stellar laser can be assumed incoherent (Gaussian). The correlation function of the intensity fluctuations $I(t)$ for such light

$$k(\tau) = \langle \Delta I(t+\tau)\Delta I(t)\rangle, \quad \Delta I(t) = I(t) - \langle I(t)\rangle \tag{13}$$

(the angle brackets denote time averaging) is related with the width $\Delta\nu$ of the spectrum by the expression

$$k(\tau) = \langle I(t)\rangle^2 |\gamma(\tau)|^2, \tag{14}$$

where $|\gamma(t)|^2 = \exp(-\tau\pi\Delta\nu)$. By measuring $k(\tau)$, we can determine $\Delta\nu$. The narrowing of the spectrum should be manifested in the appearance of correlations with the characteristic time $\tau_{cor} \approx 1/\pi\Delta\nu \gg (\Delta\nu_D)^{-1}$, where $\Delta\nu_D$ is the Doppler width of the amplifying transition. The correlation method is also advantageous for such measurements for the following reasons.

First, the narrowing of the spectrum results in the corresponding increase in the brightness temperature of emission and, therefore, in the increase in the signal-to-noise ratio (S/N). Indeed, upon observation of the intensity correlations of an incoherent source having the area Σ_s and located at a distance of R from a detector [83], the signal-to-noise ratio is

$$\frac{S}{N} = \kappa(t_r\tau_0)^{1/2}\Delta\nu\,\frac{\Sigma_s\Sigma_d}{\lambda^2 R^2}\left[\exp\left(\frac{\hbar\omega_{32}}{kT_{br}}\right) - 1\right]^{-1}, \tag{15}$$

where κ is the quantum efficiency of the detector; t_r is the measurement time; τ_0 is the delay of the correlation measurement; Σ_d is the area of the emission observation with a telescope; and T_{br} is the brightness temperature. One can see from (15) that the signal-to-noise ration strongly increases with increasing brightness temperature. The absolute value of S/N also corresponds to experimental possibilities. Indeed, for example, for $R = 10^{20}$ cm (100 light years) , $\kappa = 10^{-1}$, $t_r \approx 10^3$ s, $\Sigma_s = 4\pi r^2 \approx 10^{23}$ cm^2, $\Sigma_d \approx 10^4$ cm^2, $\Delta\nu = 10^6$ s^{-1}, $\hbar\omega_{32}/kT_{br} \approx 10^{-4}$ and $\tau_0 \approx 10^{-7}$ s, we obtain $S/N \sim 100$.

Second, when radiation is detected in two independent spatial points, the correlation method can be used for measuring the size of the lasing region, i.e., the critical radius r_0 (the Brown–Twiss method [79]). The minimum base b_0 (the distance between the observation points) required for the resolution of a source with the linear size r_0 located at a distance $R \gg r_0$ from detectors is determined by the expression [80]

$$b_0 = \frac{3.8\lambda R}{r_0}. \tag{16}$$

For example, for $\lambda = 8446$ Å, $R = 10^{20}$ cm, and $r_0 = 10^{11}$ cm, the base $b_0 \approx 5\times10^5$ cm (5 km) is required.

Such an experiment can be most conveniently performed using the heterodyne detection, as was demonstrated by Ch. Townes and co-workers in the region of 10 μm [84]. Progress in the development of tunable lasers, fibre optics, and quick-response photodetectors allows one to carry out such an experiment using the scheme shown in Fig. 15. This scheme provides simultaneously the maximum sensitivity and maximum spectral and spatial resolution. In addition, the correlation method in insensitive to the inevitable shifts of spectral lines due to different local velocities of APLs.

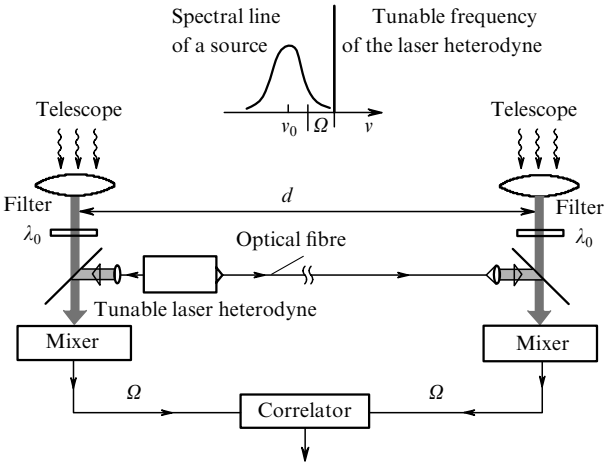

Figure 15. Scheme for the correlation measurement of the width of narrow lines of APLs by using two spatially separated telescopes and heterodyne detection with a common tunable laser heterodyne.

10. Conclusions

The astrophysical laser is a natural quantum-electronic 'device' of an extremal size, which is located at the end of the size-active laser particle density diagram shown in Fig. 16. At the diagram centre, the first laboratory masers and lasers are located. N.G. Basov made the fundamental contribution and put all his heart and soul to the discovery of these devices. At one end of the diagram, semiconductor lasers are located, which were also initiated by pioneering works of N.G. Basov and his co-workers at the dawn of quantum electronics. Due to the discovery and realisation of heterojunctions by Zh.I. Alferov [85], these lasers became the most widespread lasers in quantum electronics and its various applications. Finally, at the opposite end of the diagram, the astrophysical masers and lasers are located, in which the incoherent scattering feedback probably acts, which was also discovered in the 1960s in studies supervised

by N.G. Basov. Figuratively speaking, the scale of a huge and multidimensional personality of my teacher N.G. Basov is comparable with the scale of the diagram in Fig. 16 covering twenty orders of magnitude.

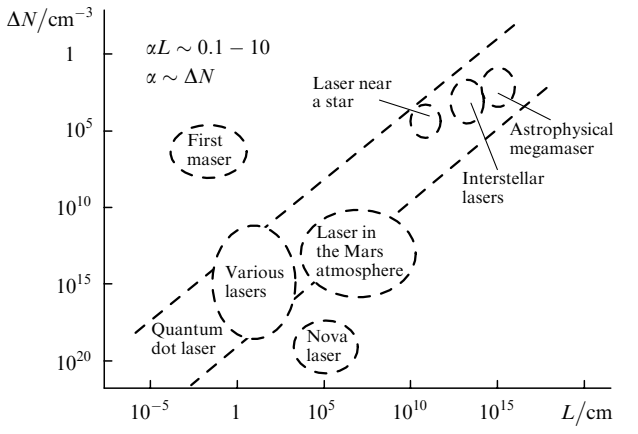

Figure 16. Various laboratory and astrophysical masers and lasers in the active medium particle density – active medium size diagram.

Acknowledgements. The author thanks Prof. S. Johansson for joint work, the results of which are used in Section 5 and information on paper [58], and A.A. Makarov, for useful comments during the preparation of the review.

References

1. Basov N.G., Prokhorov A.M., Townes C.H. *Usp. Fiz. Nauk*, **85**, 585 (1965).
2. Maiman T. *Nature*, **187**, 493 (1960).
3. Javan A., Bennett W. Jr., Herriott D.R. *Phys. Rev. Lett.*, **6**, 106 (1961).
4. Weinreb S., Meeks M.L., Carter J.C., Barrett A.H., Rogers A.E.E. *Nature*, **206**, 440 (1965).
5. Cheung A.C., Rank D.M., Townes C.H., Thornton O.D., Wehl W.J. *Nature*, **22**, 626 (1969).
6. Bowen I. *Astrophys. J.* **81** (1935).
7. Bowen I.S. *Publ. Astronom. Soc. Pacific.*, **46**, 146 (1934).
8. Thackerey A.D. *Astrophys. J.*, **81**, 467 (1935).
9. Siegman A. *Lasers* (University Science Book, 1986).
10. Woodbury G.J., Ng W.R. *Proc. IRE*, **50**, 2347 (1962).
11. Lamb W.E. Jr., Scully M.O. *Phys. Rev.*, **159**, 208 (1967).
12. Alzetta G.A., Gozzini L., Moi L., Orriols G. *Nuovo Cimento B*, **36**, 5 (1976).
13. Arimondo E. *Progress in Optics*. Ed. by E. Wolf (Amsterdam: Elsevier, 1996) Vol. XXXV, p. 25.
14. Harris S.E. *Phys. Today*, **50**, 36 (1997).
15. Zibrov A.S., Lukin M.D., Nikonov D.E., Hollberg L., Scully M.O., Velichansky V.L., Robinson H.G. *Phys. Rev. Lett.*, **75**, 1499 (1995).
16. Padmabandu G.G., Welch G.R., Shubin I.N., Fry E.S., Nikonov D.E., Lukin M.D., Scully M.O. *Phys. Rev. Lett.*, **76**, 2053 (1996).
17. Letokhov V.S. *IEEE J. Quantum Electron.*, **8**, 615 (1972); Preprint of Institute of Spectroscopy, (9) (Troitsk, 1972).
18. Johansson S., Letokhov V.S. *Pis'ma Zh. Eksp. Teor. Fiz.*, **75**, 591 (2002).
19. Gould G. *Appl. Opt. Suppl. on Chem. Las.*, **384**, 350 (1965).
20. Scmid H. *Astron. Astrophys.*, **211**, L31 (1989).
21. Sorokin P.P., Glownia J.H. *Astron. Astrophys.*, **384**, 350 (2002).
22. Unsold A. *Physik der Sternatmosphëren* (Berlin: Springer-Verlag, 1968; Moscow: Izd. Inostr. Liter., 1949).
23. Merill P. *Lines of the Chemical Elements in Astronomical Spectra* (Washington DC: Carnegie Institute of Washington, 1956; Moscow: Fizmatgiz, 1959).
24. Gorbatskii V.G. *Spektry nestatsionarnykh zvezd v teorii zvezdnykh spektrov* (Spectra of Nonstationary Stars in the Theory of Stellar Spectra) (Moscow: Nauka, 1966).
25. Sletteback A. *Astrophys. J.*, **113**, 436 (1951).
26. Bowen J.S. *Publ. Astronom. Soc. Pacific.*, **59**, 196 (1947).
27. Burbidge E.N. *Astrophys. J.*, **115**, 418 (1952).
28. Merrill P.W. *Astrophys. J.*, **114**, 37 (1951).
29. Merrill P.W. *Astrophys. J.*, **116**, 22 (1952).
30. Basov N.G., Prokhorov A.M. *Zh. Eksp. Teor. Fiz.*, **28**, 249 (1955).
31. Bloembergen N. *Phys. Rev.*, **104**, 324 (1958).
32. Letokhov V.S. *Zh. Eksp. Teor. Fiz.*, **53**, 1442 (1967).
33. Ambartzumian R.V., Basov N.G., Kriukov P.G., Letokhov V.S. *Progress in Quantum Electron.*, **1**, 107 (1971).
34. Lavrinivich N.N, Letokhov V.S. *Zh. Eksp. Teor. Fiz.*, **67**, 1609 (1974).
35. Letokhov V.S., in *Amazing Light*. Ed. by R.Y. Chiao (Berlin: Springer, 1996) pp 409 – 443.
36. Townes C.H. *Kvantovaya Elektron.*, **24**, 1063 (1997) [*Quantum Electron.*, **27**, 1031 (1997)].
37. Strelnitski V., Haas M.R., Smith H.A., Erikson E.F., Colgan S.W.J., Hollenbach D.J. *Science*, **272**, 1459 (1996).
38. Betz A.L., McLaren R.A., Sutton E.C., Townes C.H. *Astrophys. J. Lett.*, **208**, L145 (1976).
39. Mumma M.J., Buhl D., Chin G., Deming D., Espenak F., Kostink T., Zipoy D. *Science*, **212**, 45 (1981).
40. Johansson S., Davidson K., Ebbets D., Weigelt G., Balick B., Frank A., Haman F.H., Humphreys R.M., Morse J., White R.L., in *Science with Hubble Space Telescope-II*. Ed. by R. Benvenutti, F.D. Macchetto, E.J. Schreiew (Paris: ESA, 1996) p. 361.
41. Johansson S., Letokhov V. *Astron. Astrophys.*, **378**, 266 (2001).
42. Klimov V., Johansson S., Letokhov V. *Astron. Astrophys.*, **385**, 313 (2002).
43. Schawlow A.L., Townes C.H. *Phys. Rev.*, **112**, 1940 (1958).
44. Kimble R.A., et al. *Astrophys. J.*, **492**, L83 (1998).
45. Gull T.R., Ishibashi K., Davidson K., in *Eta Carinae at the Millenium*. Ed. by J.A. Morse, R.M. Humphreys, A. Damineli (ASP Conf. Ser., 1999) Vol. 179, p. 144.
46. Weigelt G., Ebersbergen J. *Astron. Astrophys.*, **163**, L5 (1986).
47. Davidson K., Humphreys R.M. *Ann. Rev. Astron. Astrophys.*, **35**, 1 (1997).
48. Stromgren B. *Astrophys. J.*, **89**, 526 (1932).
49. Gull T., Ishibashi K., Davidson K., Collins N., in *Eta Carinae and Other Mysterious Stars*. Ed. by T. Gull, S. Johansson, K. Davidson (ASP Conf. Ser., 2001) Vol. 242, p. 391.
50. Johansson S., Jordan C. *Mon. Not. R. Astr. Soc.*, **210**, 239 (1984).
51. Johansson S., Hammann F. *Phys. Scripta*, **47**, 157 (1993).
52. Johansson S., Zethson T., Hartman H., Letokhov V., in *Eta Carinae and Other Mysterious Stars*. Ed. by T. Gull, S. Johansson, K. Davidson (ASP Conf. Ser., 2001) Vol. 242, p. 297.
53. Bennett W.R. Jr., Faust W.L., McFarlane R.A., Patel C.K.H. *Phys. Rev. Lett.*, **8**, 470 (1962).
54. Sobel'man I.I., Vainshtein L.A., Yukov E.A. *Excitation of Stars and Broadening of Spectral Lines* (Berlin: Springer-Verlag, 1981).
55. Allen C.W. *Astrophysical Quantities* (London: Athlone Press, 1973; Moscow: Mir, 1977).
56. Boyarchuk A.A. *Astron. Zh.*, **34**, 193 (1957).
57. Mustel E.R. *Astron. Zh.*, **18**, 297 (1941); **21**, 133 (1944).
58. Münch G., Taylor K. *Astrophys. J.*, **192**, L93 (1974).
59. Gull T., Goad L., Chin N.-Y., Maran S.P., Hobbs R.W. *Publ. Astronomic. Soc. Pacific*, **85**, 526 (1973).
60. Casperson L.W., Yariv A. *IEEE J. Quantum Electron.*, **8**, 80 (1972).
61. Allen L., Peters G.I. *Nature. Phys. Sciences*, **235**, 143 (1972).
62. Litvak M.M. *Phys. Rev. A*, **2**, 2107 (1970).
63. Cook A.H. *Celestial Masers* (Cambridge: Cambridge Univ. Press, 1977).
64. Reid J.J., Moran J.M. *Ann. Rev. Astron. Astrophys.*, **19**, 231 (1981).

65. Elitzur M. *Rev. Mod. Phys.*, **54**, 1225 (1982).
66. Barrett A.H., Rogers A.E.E. *Nature*, **210**, 188 (1966).
67. Letokhov V.S., Chebotaev V.P. *Nonlinear Laser Spectroscopy* (Berlin: Springer-Verlag, 1976; Moscow: Nauka, 1990).
68. Prokhorov A.M. *Zh. Eksp. Teor. Fiz.*, **34**, 1658 (1958).
69. Ambartzumian R.V., Basov N.G., Kryukov P.G., Letokhov V.S. *Pis'ma Zh. Eksp. Teor. Fiz.*, **51**, 274 (1966); *IEEE J. Quantum. Electron.*, **2**, 442 (1966).
70. Ambartzumian R.V., Basov N.G., Kryukov P.G., Letokhov V.S. *Progress in Quantum Electronics*. Ed. by K.W.N. Stevens, J.H. Sanders (London: Pergamon Press, 1970) Vol. 1, p. 105.
71. Ambartzumian R.V., Kryukov P.G., Letokhov V.S. *Zh. Eksp. Teor. Fiz.*, **51**, 1669 (1966).
72. Ambartzumian R.V., Kryukov P.G., Letokhov V.S., Matveetz Yu.A. *Pis'ma Zh. Eksp. Teor. Fiz.*, **5**, 378 (1967); *Zh. Eksp. Teor. Fiz.*, **53**, 1955 (1967).
73. Letokhov V.S. *Zh. Eksp. Teor. Fiz.*, **53**, 2110 (1967).
74. Letokhov V.S. *Pis'ma Zh. Eksp. Teor. Fiz.*, **5**, 262 (1967); *Zh. Eksp. Teor. Fiz.*, **53**, 1442 (1967).
75. Lawandy N.M., Balachandran R.M., Gomes A.S.L., Sauvarn E. *Nature*, **368**, 436 (1994).
76. Markushev V.M., et al. *Kvantovaya Elektron.*, **13**, 427 (1986) [*Sov, J. Quantum Electron.*, **16**, 281 (1986)]; **17**, 854 (1990) [*Sov, J. Quantum Electron.*, **20**, 773 (1990)]; Cao H., Xu S.T., Chang S.-H., Ho S.T. *Phys. Rev.*, **61**, 1985 (2000).
77. Letokhov V.S. *Pis'ma Zh. Eksp. Teor. Fiz.*, **4**, 477 (1966); *Astron. Zh.*, **49**, 737 (1972).
78. Truitt P., Strelnitskii V. *Meeting 197 Amer. Astronom. Soc.* (January, 2001).
79. Hanberry Brown R., Twiss R.Q. *Proc. Roy. Soc. A*, **242**, 300 (1957); **243**, 291 (1958); **248**, 199 (1958).
80. Mandel L. *Progress in Optics*. Ed. by E. Wolf (Amsterdam: Elcevier, 1963) Vol. 2, p. 181.
81. Lavrinovich N.N., Letokhov V.S. *Kvantovaya Elektron.*, **3**, 1948 (1976) [*Sov. J. Quantum Electron.*, **6**, 1061 (1976)].
82. Dravins D., in *Eta Carinae and Other Mysterious Stars*. Ed. by T. Gull, S. Johansson, K. Davidson (ASP Conf. Ser., 2001) Vol. 339.
83. Goldberger M.L., Lewis H.W., Watson K.M. *Phys. Rev.*, **142**, 25 (1966).
84. Johnson M.A., Betz A.L., Townes C.H. *Phys. Rev. Lett.*, **33**, 1617 (1974).
85. Alferov Zh.I. *Rev. Mod. Phys.*, **73**, 767 (2001).

N.G. Basov, Ch. Townes, A.M. Prokhorov at the FIAN, 1965.